ISSN 2070-0466, p-Adic Numbers, Ultrametric Analysis and Applications, 2013, Vol. 5, No. 4, pp. 260–277. © Pleiades Publishing, Ltd., 2013.

RESEARCH ARTICLES

Storage and Retrieval of Ultrametric Patterns in a Network of CA1 Neurons of the Hippocampus*

D. Bianchi[1], **M. Piersanti[1]**, and **B. Tirozzi[1]**

[1] *Department of Physics, 'Sapienza' University of Rome, Italy*

Received September 29, 2013

Abstract—We explore the possibility of storage and retrieval of ultrametrically organized patterns in hippocampus, the part of the brain devoted to the memory processes. The ultrametric structure has been chosen for having a good representation of the categories of memory. The storage and retrieval process is the one typical of the hippocampus and it is based on the dynamic of the CA1 neurons under the input from the neurons of the Enthorinal cortex and the Ca3 system. We explore if this real system of neurons exhibits the property of associative memory introduced since a long time in the artificial neural networks. We study how the performance is dependent on the deviation of the system of patterns from ultrametricity. The evolution of the system is simulated by means of a parallel computer and the statistics of storage and retrieval is investigated.

DOI: 10.1134/S207004661304002X

Key words: *CA1 neurons, associative memory, ultrametric patterns.*

1. INTRODUCTION

Ultrametricity has been introduced as a generalization of the Euclidean metric and used for a long time as an instrument of analysis of differential operators, pseudo-differential operators and geometric properties. The development of the analysis of the disordered systems of statistical mechanics brought to the scientific community the evidence that the non-euclidean metric is intrinsic to the space of extremal measures of Gibbs states of the spin glass [15].

Spin glass describes a physical lattice system of Copper atoms with random impurities. The discovery of the ultrametric structure of the probability states associated to this system suggested immediately that the extremal states, i.e. the physical observable states of these systems have a non-euclidean distance satisfying the ultrametric inequality. These systems are composed by a large number of units, the spins of the atoms, which take values ± 1. Thus the statistical mechanics of the disordered alloys gave evidence that observed states of sequences of random variables ± 1 satisfy a non trivial distance inequality.

The Hopfield model has been formulated and solved in [2, 18] after the solution of the spin-glass model. This model is closer to the object of this work because the ± 1 variables have the meaning of neural activities and the sequences of such variables represent a set of information. The Hopfield model mimics the storage and retrieval of information and is also a disordered system, so it is natural that its extremal states have an ultrametric structure. But ultrametricity is also a natural framework for describing group of concepts classified with categories, ancestors and descendants.

It has been shown that the Hopfield model can store and retrieve patterns grouped ultrametrically into categories (Section 2). Our attempt is to store and retrieve patterns of the same type into a system of real neurons of the Hippocampus (CA1). Thus we are trying to apply the methods

[0] Based on talk at the *International Workshop on p-Adic Methods for Modelling of Complex Systems*, Bielefeld, April 15–19, 2013.

[*] The text was submitted by the authors in English.

[**] E-mail: danielabianchi12@gmail.com

[***] E-mail: m.piersanti@gmail.com

[****] E-mail: b.tirozzi@libero.it

of associative memory in a real system of neurons which are involved with the memory process in humans and animals. We adapt the model of the network of CA1 neurons of [5] to our case: first we substitute the CA1 model with a model which exhibits the depolarization block [4] and we study the storage and retrieval of ultrametric patterns in the presence of CREB or not. CREB is a special protein which increases the neural activity, as it has been revealed in experiments [13]. So we study how the memory works in the Hippocampus, both in presence of CREB and without it (Control case) and we find how storage and recall depend on the ultrametric structure of the set of patterns.

In other words we study the dependence of the memory functions on the degree of categorization of the information to be stored. We also find (Section 5) the dependence of the recall quality on the degree of ultrametricity. In Section 2 we explain the models of associative memory and how the ultrametric structure can be put inside them, in Section 3 we show how one can define the parameters which measure the degree of ultrametricity. In Section 4 we describe the network of the CA1 neurons and in Section 5 we finally give the results.

2. ULTRAMETRIC PATTERNS IN ASSOCIATIVE MEMORY MODELS

2.1. Associative memory and Hopfield model

Associative memory is the ability of humans of remembering an information starting from a partial knowledge of it. For example, remembering the entire title of a film knowing only a part of it. The first question that arises is how to learn patterns and conserve them, i.e. learning and storage. Once some patterns have been learned and stored the fundamental ability is to retrieve them.

In the last 30 years a lot of work, both theoretical and experimental, has been done to construct models of associative memory. The important feature of these models is a measure of the retrieval and storage. The models are built with a number N of units, called *neurons*, and a number p of information called *patterns*. This measure is called *capacity* and is defined as the ratio

$$\alpha = \frac{p}{N}. \tag{2.1}$$

The first attempt to simulate the behavior of human long-term memory was the Hopfield model [10]. The units were called neurons since their functioning was mimicking the dynamics of real neurons, the set of N neurons was called *neural network*. The neurons were represented as an idealized two-state devices [14], coupled through a symmetrical matrix J_{ij}. Real neurons are coupled through very thin tubes called dendrites which end on the membrane of the adjacent neuronal cell in a structure called synapses.

The learning process is a particular evolution of the synaptic matrix J_{ij}, often a stochastic process, which makes the matrix to converge to some definite matrix which allows the retrieval of the information. The learning process is called *supervised* if the evolution is controlled by some external factor, *unsupervised* if there is no form of external control during the evolution.

Here we summarize the basic assumptions and definitions of the Hopfield model.

- The *all-or-none* firing of a neuron is represented by a variable S_i taking two values: $S_i = +1$ (firing), $S_i = -1$ (rest). There are N of such variables. A configuration of the system is a collection of these variables $\underline{S} \equiv (S_1, S_2, \dots, S_N)$.

- The dynamics of a neuron is a stochastic threshold dynamics:

$$S_i(t+1) = \operatorname{sgn} h_i(t), \tag{2.2}$$

$$h_i(t) = \sum_{j,\, j \neq i}^{N} J_{ij} S_j(t). \tag{2.3}$$

- A pattern of activity, $\underline{\xi}^{\mu}$, of a network of N neurons is represented by a set of i.i.d.r.v. $\{\xi_i^{\mu} = \pm 1\}$, $i = 1, \dots, N$, that lies at the corners of an N dimensional hypercube. There are p patterns $\underline{\xi}^{\mu}$ to store and retrieve, $\mu = 1, \dots, p$.

- Two patterns of activity, μ and ν, may be compared through their *overlap*:

$$\langle \mu|\nu\rangle = \frac{1}{N}\sum_{i=1}^{N}\xi_i^\mu\xi_i^\nu. \tag{2.4}$$

- The overlap m^μ of a pattern $\underline{\xi}^\mu$ with a configuration $\underline{S}$ is a measure of the retrieval of the stored information in the network

$$m^\mu = \frac{1}{N}\sum_{i=1}^{N}\xi_i^\mu S_i. \tag{2.5}$$

- During learning the $J_{\rm ij}$ are modified by the system. A set of p patterns $\{\xi_i^\mu\}$ is embedded in the J_{ij}'s via the *Hebbian* learning rule

$$J_{ij} = \frac{1}{N}\sum_{\mu=1}^{p}\xi_i^\mu\xi_j^\mu. \tag{2.6}$$

  The learning process of the Hopfield model is a supervised process.

- The patterns are memorized in the sense that each pattern $\underline{\xi}^\mu$ is a fixed point of the dynamics.

The result of the investigations made by [2, 10] was that there is critical value of the capacity α_c such that all the overlap parameters are zero for $\alpha > \alpha_c$. The value found was $\alpha_c \sim 0.134$.

2.2. Classes of patterns and ultrametricity

The memorization and retrieval of information is easier if one uses classes. Classes are like atoms of a partition of a finite set, the single pattern being an element of the atom. The hierarchical structure of the patterns is thus well described using the ultrametric distance in an ultrametric space.

Marc Krasner (1912–1985) invented this word in a note presented at the French Academy of Sciences on October 23, 1944, entitled "Nombres semi-réels et espaces ultramétriques".

The *ultrametric inequality* is the inequality:

$$d\left(A,C\right) \leq \max\left\{d\left(A,B\right),\, d\left(B,C\right)\right\}. \tag{2.7}$$

A distance that satisfies the ultrametric inequality is called an *ultrametric distance*. A space endowed with an ultrametric distance is called an *ultrametric space*.

The problem is then to organize the patterns in such a way that they are divided in classes and elements of the classes, and distinguish among them by means of a distance, which is the ultrametric distance.

The aim is to construct patterns which have an ultrametric structure and such that they can be used for storage and retrieval in a network of real neurons. There are many ways to organize patterns in an ultrametric space.

2.3. Ultrametric patterns in the Hopfield model

Definition 2.1 (Ancestors)**.** *p patterns $\{\xi^\mu = \pm 1\}$ with $\mu = 1, \ldots, p$, ξ^μ being IIDRV.*

Definition 2.2 (Descendants)**.** *Each ancestor has q_μ descendants $\{\xi^{\mu,\nu}\}$ (see Fig. 1).*

$$\xi_i^{\mu,\nu} = \xi_i^\mu\eta_i^{\mu,\nu} \tag{2.8}$$

with

$$Pr(\eta^{\mu,\nu} = \pm 1) = \frac{1}{2}(1 \pm a_\mu). \tag{2.9}$$

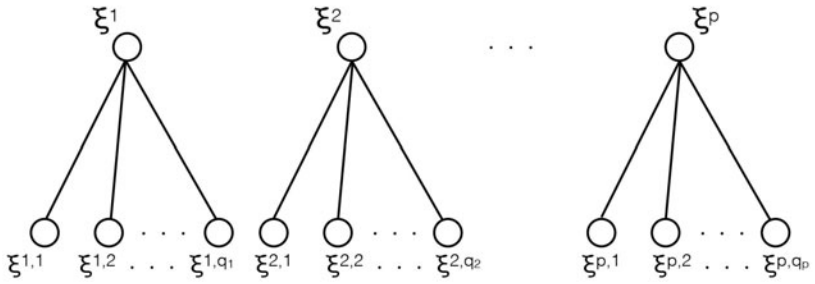

Fig. 1. A two level tree with different ancestors.

- Two patterns in the same bunch have overlap < 1 (since $a_\mu < 1$)

$$\langle \mu, \nu | \mu, \lambda \rangle \equiv \frac{1}{N} \sum_{i=1}^{N} \xi_i^{\mu,\nu} \xi_i^{\mu,\lambda} = \frac{1}{N} \sum_{i=1}^{N} \eta_i^{\mu,\nu} \eta_i^{\mu,\lambda} = a_\mu^2. \tag{2.10}$$

- Two patterns in different bunches have overlap equal to 0

$$\langle \mu, \nu | \rho, \lambda \rangle = 0. \tag{2.11}$$

At this stage we have ultrametricity. If we choose any three states which are either in one bunch or in three separate bunches, then they are equidistant. If two are in one bunch and the third is in a separate one, then two distances are maximal (the overlap is 0) and one distance is less than 1.

The synaptic matrix that stabilises these patterns is

$$T_{ij} = \frac{1}{N} \sum_{\mu=1}^{p} \xi_i^\mu \xi_j^\mu \left(1 + \frac{1}{\Delta} \sum_{\nu=1}^{q_\mu} (\eta_i^{\mu,\nu} - a_\mu)(\eta_j^{\mu,\nu} - a_\mu) \right). \tag{2.12}$$

- When $\Delta = 1 - a^2$, the degeneracy between parents and descendants sets in. The storage capacity is the familiar $\alpha \approx 0.15$, where α refers to the total number of memorized pattern, i.e.

$$\alpha N = p + \sum_{\mu=1}^{p} q_\mu. \tag{2.13}$$

  All these states become attractors.

- If $\Delta > 1 - a^2$ the degeneracy is lifted and the parents become lower in energy than the descendants.

- The total storage capacity remains the same, but the ancestors appear first, at higher loading levels, and then the detailed descendants become retrieval states at lower loading levels.

3. DEVIATIONS FROM ULTRAMETRICITY

3.1. Rammal index

Let E be a finite set. A *hierarchy* $\hat{H}$ on E is a special set of partitions of E, $\hat{H}(E)$, such that

i) $E \in \hat{H}(E)$;

ii) each single element $a \in E$ belongs to $\hat{H}(E)$, i.e. the atoms of the partitions can be also single elements (singleton);

iii) for each pair of partitions $r, r' \in \hat{H}$, such that $r \cap r' \neq 0 \Longrightarrow r \subset r'$ or $r' \subset r$

An *indexed hierarchy* on E is a pair $\{\hat{H}, f\}$ where $\hat{H}$ is a given hierarchy on E and f is a positive function satisfying the following conditions

i) $f(a) = 0$ if and only if a is a single element of E (a singleton);

ii) if $a \subset a'$ then $f(a) < f(a')$.

f corresponds to the index of the levels of the hierarchies introduced in Section 2.

The distance among two subsets of E is

$$\delta(a, b) = \min\{d(x, y) \,|\, x \in a,\, y \in b\}. \tag{3.1}$$

Example 3.1 (Trivial ultrametric)**.** *If $E : E = \cup_i E_i$, then $d(x, x) = 0$, $d(x, y) = 1$ if $x \in E_i$, $y \in E_j$ $(i \neq j)$, and $d(x, y) = a$ if $i = j$, $0 < a < 1$.*

Associated with each indexed hierarchy $\{\hat{H}(E), f\}$ on E is the following ultrametric:

$$\sigma(x, y) = \min_{a \in \hat{H}(E)} \{f(a) \,|\, x \in a,\, y \in a\}. \tag{3.2}$$

This means that the distance $\sigma(x, y)$ between two elements x and y in E is given by the index of the smallest element in $\hat{H}(E)$, which contains both x and y (rule of the closest common ancestor).

The measure of approximation of the measure d (proximity index) is

$$\Delta_0(d, \delta) = \max_{x,y \in E} |d(x, y) - \delta(x, y)|. \tag{3.3}$$

Our goal is then to find the best approximating $\delta(x, y)$ of $d(x, y)$.

Limit the search on a subset of $\mathcal{U}$ (the set of all the ultrametrics on E):

$$\mathcal{U}^s = \{\delta \in \mathcal{U} \,|\, \delta \leq d\}. \tag{3.4}$$

The *subdominant ultrametric* d^s is defined as the upper limit of $\mathcal{U}^s$. This is the maximal element in $\mathcal{U}^s$, and by definition

$$d^s(x, y) = \max\{\delta(x, y) \,|\, \delta \in \mathcal{U}, \delta \leq d\}, \tag{3.5}$$

$$\Delta(d, d^s) = \min\{\Delta(\delta, d) \,|\, \delta \in \mathcal{U}, \delta \leq d\}. \tag{3.6}$$

We use the *Minimum-Spanning-Tree* (MST) construction method [16, 21].

Note that although the MST is not uniquely defined, d^s is unique.

If A is a MST on E, the distance $d^s(x, y)$ between two elements x and y in E is given by

$$d^s(x, y) = \max\{d(w_i, w_{i+1}), i = 1, \ldots, n-1\}, \tag{3.7}$$

where $\{(w_1, w_2), (w_2, w_3), \ldots, (w_{n-1}, w_n)\}$ denotes the unique chain in A, between x and y ($w_1 = x$, $w_n = y$). An example of this construction is depicted in Fig. 2.

Definition 3.2 (Distortion index)**.**

$$\mathcal{D} = 1 - \frac{\sum_{x,y \in E} d^s(x, y)}{\sum_{x.y \in E} d(x, y)}, \tag{3.8}$$

where d is the input metric on E, d^s is the associated subdominant ultrametric.

In general, $0 \leq \mathcal{D} \leq 1$, vanishes if d is already an ultrametric (i.e., $d^s = d$) and provides a quantitative measure of ultrametricity.

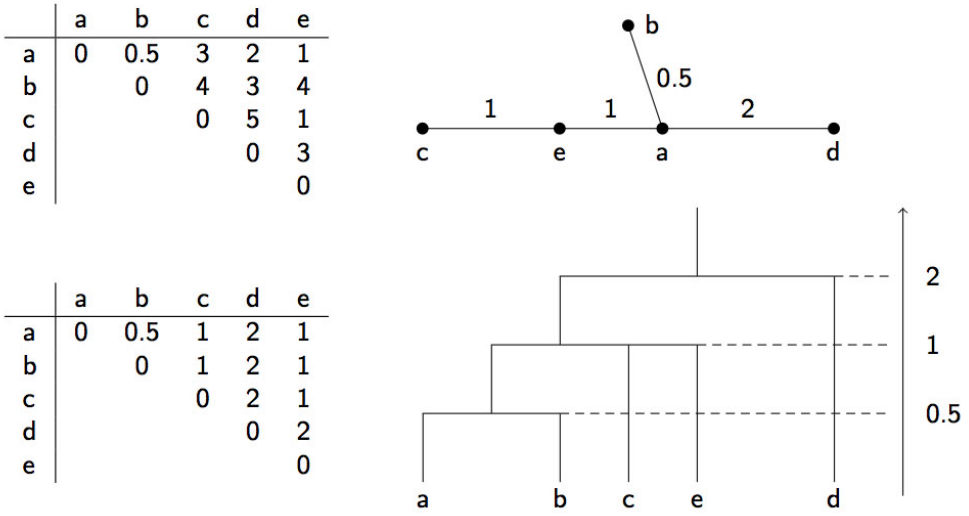

Fig. 2. An illustrative example of the construction of the subdominant ultrametric d^s (bottom) on the metric space (E, d) of five elements, using the method of the minimum-spanning tree (MST).

Example 3.3. *Take* $E = \{x_1, \ldots, x_n\}$, $x_i \in R$ *and* $d(x_i, x_j) = |x_i - x_j|$ *is the usual Euclidean metric. If* $x_i = i$, *then the MST is the set of edges going from* x_i *to* $x_{i+1} \to d^s(x_i, x_j) = 1$*: all triangles are equilateral. It can be shown that for large* n

$$\mathcal{D} \simeq 1 - \frac{3}{n+1} \sim 1. \tag{3.9}$$

Euclidean spaces are far from being ultrametric spaces.

Example 3.4. *Let* E *be a set of* P *binary words of* N *bits each, taken randomly from among the* 2^N *possible words. The distance among two words* $\xi^1 = (\xi^1_1, \ldots, \xi^1_N)$, $\xi^2 = (\xi^2_1, \ldots, \xi^2_N)$ *is the Hamming distance*

$$d(\xi^1, \xi^2) = \sum_{i=1}^{N} |\, \xi^1_i - \xi^2_i \,| \tag{3.10}$$

- *for* $P = 2^N$, d^s *reduces to the trivial ultrametric and* $\mathcal{D}_{\mathcal{N}}(x = 1) = 1 - 2/N \sim 1$ *at large* N *where* $x = P/2^N$ *is the filling factor of the hypercube of all the configurations* $\{0, 1\}^N$.
- *For fixed but large* N *numerical calculations show that* $\mathcal{D}_{\mathcal{N}}$ *approaches zero as* x *goes to zero. This means that if the number of patterns is small (10 or 20) and the dimension of the vector is large (say* 100*) we have ultrametricity. Ultrametricity holds then in case of large spaces (*sparse coding*), that is the case of the patterns of the CA1 neural activity.*

3.2. Lerman index

A preorder can be associated to a set of partitions organized in a lattice $\hat{P}(E)$. Let F be the set of all pairs of elements in E. The distance d defines a *total preorder* in F:

$$\forall\{(x, y), (z, t)\} \in F : (x, y) \leq (z, t) \iff d(x, y) \leq d(z, t). \tag{3.11}$$

The preorder is indicated with ω. Two distances on a given set E are equivalent if the preorderings associated with each of them on E are identical. A total preorder is equivalent to a partition which defines an equivalence relation on F, and to a total order on the set of classes.

A preorder ω is called ultrametric if

$$\forall x, y, z \in E : \rho(x, y) \leq r\ ,\ \rho(y, z) \leq r \Longrightarrow \rho(x, z) \leq r, \tag{3.12}$$

where $\rho(x, y)$ is the rank of the pair, for ω defined by the non-decreasing values of the distance d in E.

A necessary and sufficient condition for a distance d to be ultrametric is that the associated preordering is ultrametric.

It is possible to introduce a quantity which measures the degree of ultrametricity starting from these definitions. Let J be the set of all the triplets (x, y, z) of elements of E. Consider the application τ of J in F that, given (x, y, z) and the preorder ω, associates to them the open interval $]M(x, y, z), S(x, y, z)[$, which are respectively the median and the maximum among the three couples (x, y), (y, z) and (z, x).

We just say that a triplet (x, y, z) for which $(x, y) \leq (y, z) \leq (x, z)$, given the preordering ω, is such that the interval $](y, z), (x, z)[$ is empty if ω is ultrametric. Considering such a triplet, the preorder ω is less and less ultrametric as the cardinality of $](y, z), (x, z)[$ become bigger. To take into account the set J of all the triplets, we may adopt as a measure of the discrepancy between ω and an ultrametric preorder:

$$H(\omega) = \frac{1}{|J|} \sum_{J} \frac{|]M(x, y, z), S(x, y, z)[|}{|F|}, \tag{3.13}$$

where we have normalized with number of the triples $|J|$ and with the number of the pairs $|F|$.

Example 3.5. *Let $E = \{a, b, c, d, e\}$, and ω the preorder on E*

$$\{a, d\} = \{a, c\} < \{a, e\} < \{c, e\} < \{b, d\} = \{c, d\} < \{b, c\} < \{d, e\} < \{a, b\} < \{b, e\}.$$

J \ F	(a,d)	(a,c)	(a,e)	(c,e)	(b,d)	(c,d)	(b,c)	(d,e)	(a,b)	(b,e)
(a,b,c)		•					•	×	•	
(a,b,d)	•				•		×	×	•	
(a,b,e)			•						•	•
(a,c,d)	•	•	×	×		•				
(a,c,e)		•	•	•						
(a,d,e)	•		•	×	×	×	×	•		
(b,c,d)					•	•	•			
(b,c,e)				•			•	×	×	•
(b,d,e)					•			•	×	•
(c,d,e)				•		•	×	•		

Table 1. Calculating the Lerman index $H(\omega)$ for this example. On each row, a "•" indicates the pairs contained in the triple and a "×" the pairs which are strictly between the median and the maximum.

In Table 1 we reported on the rows the set of the triples J and on the columns the set of the pairs F. On each row, a "•" indicates the pairs contained in the triple and a "×" the pairs which are strictly between the median and the maximum. If there are no crosses the median and the maximum are in the same class and the preordering is ultrametric, hence $H(\omega) = 0$. Summing the number of crosses for the pairs which are strictly included between some median and maximum one obtains a quantitative measure of the deviation of (E, ω) from the ultrametric preordering.

$H(\omega)$ is a more reliable measure of the deviation from ultrametricity than the the distortion index of the subdominant metric introduced before because the subdominant metric can be very different from the metric d.

The structure of $H(\omega)$ suggests to define a measure on the space F introducing the number of pairs in F which are strictly included in the interval $]M(x,y,z), S(x,y,z)[$. Given any pair $p \in F$, we define the subset J_p of J such that, for any triple $\{x,y,z\} \in J_p$, p is strictly included in the interval $]M(x,y,z), S(x,y,z)[$. It is possible then to define a measure m_p on the space of pairs F such that for any $p \in F$

$$m_p = \frac{|J_p|}{|J|}. \tag{3.14}$$

For any preorder ω we can then define the vector $D(\omega)$ as the set of $m_p, p \in F$. If the preorder is ultrametric this vector has all the components equal to 0. Thus the number of components of $D(\omega)$ which are different from zero and also the values of these components are a measure of the deviation from ultrametricity of the preorder ω.

In this example we have that

$$H(\omega) = \frac{13}{10 \times 10}, \tag{3.15}$$

$$D(\omega) = (0.3, 0.3, 0.2, 0.2, 0.1, 0.1, 0.1, 0, 0, ...). \tag{3.16}$$

For large n, the number of elements of E, and for a large sample Q of sets of triples J obtained by generating the triples with uniform probability, we have that the $H(\omega)$ has a gaussian distribution since is the sum of indipendent uniformly distributed random variables:

$$H'(\omega) = \frac{1}{|Q|} \sum_{\{x,y,z\} \in Q} \Lambda(x,y,z), \tag{3.17}$$

where $\Lambda(x,y,z)$ is the cardinality of $]M(x,y,z), S(x,y,z)[$.

Example 3.6. *Consider a set of 6 patterns, organized in a hierarchy as described in Section 2, with 2 ancestors and 2 descendants for each ancestor.*

Then we can calculate the quantities introduced so far.

```
Minimum-spanning-tree

2 -> 0 : 12
0 -> 1 : 14
1 -> 5 : 47
5 -> 3 : 17
3 -> 4 : 14

Deviation from ultrametricity (Rammal index): 0.00788955

Preorder \omega

(0,1): 14
(0,2): 12
(0,3): 47
(0,4): 47
(0,5): 47
(1,2): 14
(1,3): 47
(1,4): 47
(1,5): 47
(2,3): 47
(2,4): 47
(2,5): 47
(3,4): 14
(4,5): 17

--> (0,2)<(0,1)=(1,2)=(3,4)<(4,5)=(0,3)=(0,4)=(0,5)=(1,3)=(1,4)=(1,5)=(2,3)=(2,4)=(2,5)
    =(3,5)
```

As one can see in Table 2, in this case the deviation from ultrametricity – Lerman's $H(\omega)$ – is 0, meaning that the space is already ultrametric.

J \ F	(0,2)	(0,1)	(1,2)	(3,4)	(4,5)	(0,3)	(0,4)	(0,5)	(1,3)	(1,4)	(1,5)	(2,3)	(2,4)	(2,5)	(3,5)
(0,1,2)	•	•	•												
(0,1,3)		•				•	–	–	•						
(0,1,4)		•					•	–	–	•					
(0,1,5)		•						•	–	–	•				
(0,2,3)	•					•	–	–	–	–	–	•			
(0,2,4)	•						•	–	–	–	–	–	•		
(0,2,5)	•							•	–	–	–	–	–	•	
(0,3,4)				•		•	•								
(0,3,5)						•		•	–	–	–	–	–	–	•
(0,4,5)					•		•	•							
(1,2,3)			•						•	–	–	•			
(1,2,4)			•							•	–	–	•		
(1,2,5)			•								•	–	–	•	
(1,3,4)				•					•	•					
(1,3,5)									•		•	–	–	–	•
(1,4,5)					•					•	•				
(2,3,4)				•								•	•		
(2,3,5)												•		•	•
(2,4,5)					•								•	•	
(3,4,5)				•	•	–	–	–	–	–	–	–	–	–	•

Table 2. Calculating $H(\omega)$ for the patterns organized hierarchically. We indicate with a "–" the lack of values in the interval $]M(x,y,z), S(x,y,z)[$.

4. ASSOCIATIVE MEMORY IN THE HIPPOCAMPUS

4.1. Our model of associative memory in CA1

The principal excitatory cells of the CA1 region are pyramidal cells (PCs). These cells are driven by excitatory inputs from layer III of the entorhinal cortex (EC) and the CA3 Schaffer collaterals and an inhibitory input from the medial septum (Sep). Recurrent connectivity between pyramidal cells is negligible in CA1 (less than 1%).

Gamma frequency rhythms (30–100 Hz) are assumed to constitute a basic clock cycle such that patterns of activity for storage and recall correspond to PCs that are active in a particular gamma cycle.

The model consists of 100 pyramidal (P) cells, 2 basket (B) cells, 1 bistratified (BS) cell, 1 axo-axonic (AA) cell, and 1 oriens lacunosum moleculare (OLM) cell (see Fig. 3).

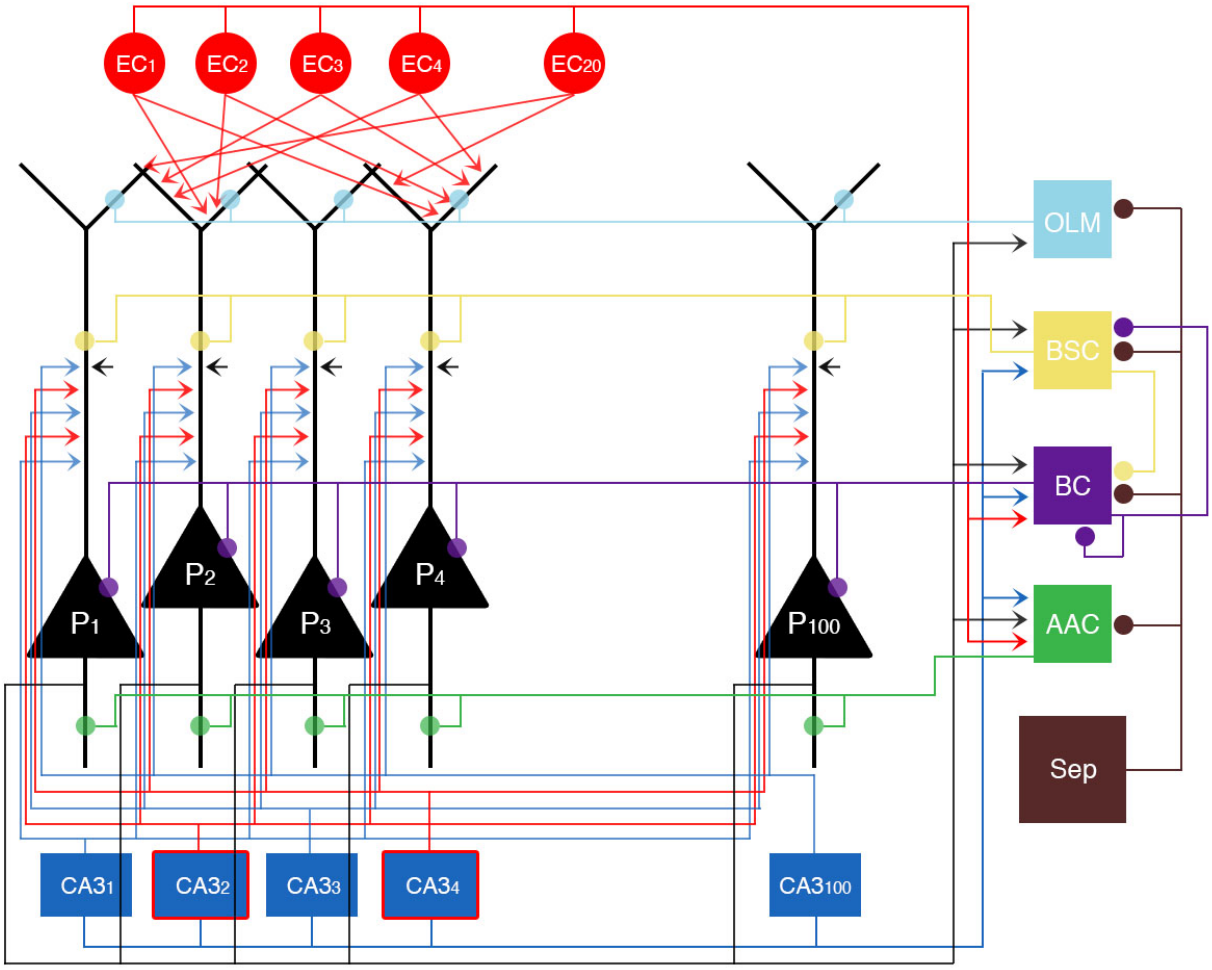

Fig. 3. *Arrows* stands for excitatory synapses, *circles* for inhibition. $P_1 ... P_{100}$: pyramidal cells. $EC_1 ... EC_{20}$: entorhinal cortex input; $CA3_1 ... CA3_{100}$: CA3 Schaffer collateral input; OLM: oriens lacunosum-moleculare cell; BSC: bistratified cell; BC: basket cell; AAC: axo-axonic cell; Sep: Septal GABA inhibition.

All cell morphologies included a soma, apical and basal dendrites and a portion of axon. The biophysical properties of each cell were adapted from cell types reported in literature [4, 19, 20, 22, 23].

Each kind of interneuron has a specific function in modulating not only the overall network functions, but also the I/O properties of the principal neurons (the CA1 pyramidal neurons) and, especially, the synaptic plasticity processes leading to memory storage. For the neurons OLM, BC, BSC and AAC the models defined for the networks of [5] are employed. The CA1 model employed, instead, has the same morphology of the CA1 template used by [5] but different distributions of the ionic currents ([4], ModelDB acc.n. 143719), in order to reproduce the depolarization block observed in these neurons. This model has been already used for simulating the storage/retrieval [3]. A schematic representation of the model cells is depicted in Fig. 4.

In the model, AMPA, NMDA, $GABA_A$ and $GABA_B$ synapses are considered. $GABA_A$ is present in all strata, whereas $GABA_B$ is present in medium and distal SR and SLM dendrites. AMPA synapses are present in strata LM (EC connections) and radiatum (CA3 connections), whereas NMDA are present only in stratum radiatum (CA3 connections).

The EC input is modeled as the firing of 20 entorhinal cortical cells at an average gamma frequency of 40 Hz (spike trains only modeled and not the explicit cells), and the CA3 input is modeled with the same gamma frequency spiking of 20 out of 100 CA3 pyramidal cells. PCs,

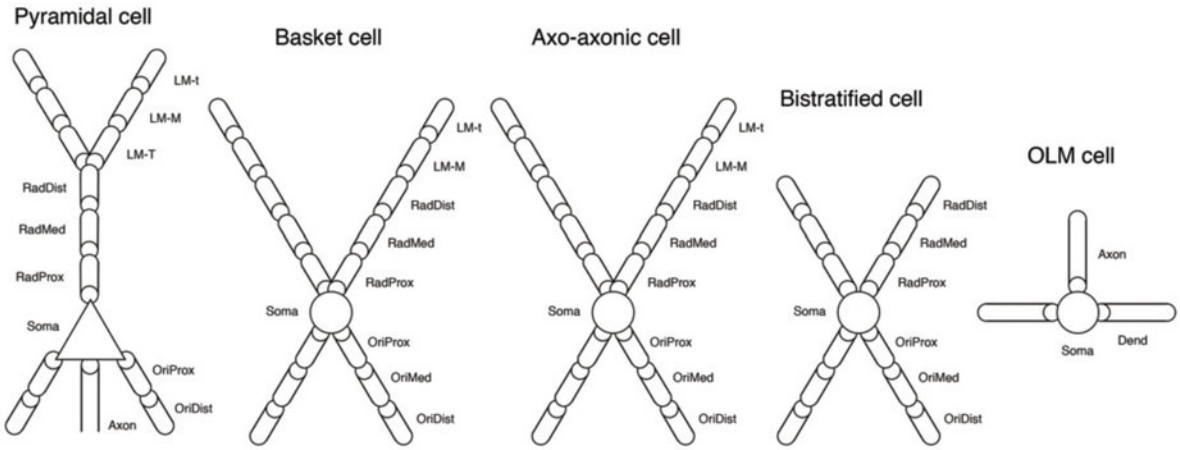

Fig. 4. Compartmental structure models for the different cell types. LM-t: lacunosum moleculare thin compartment; LM-M: lacunosum moleculare medium compartment; LM-T: lacunosum moleculare thick compartment; OriProx: oriens-proximal compartment; OriMed: oriens medial compartment; OriDist: oriens distal compartment; RadProx: radiatum proximal compartment; RadMed: radiatum medial compartment; RadDist: radiatum distal compartment; Dend: basal OLM cell compartment.

BCs, AACs, BSCs received CA3 input in their medial SR dendrites, whereas PCs, BCs and AACs received also the EC layer III input in their apical LM dendrites. EC inputs preceded CA3 inputs by 9 ms on average [24]. MS input, which is modeled as the rhythmic firing of 10 septal cells, provides $GABA_A$ inhibition to all interneurons in the model (strongest to BC and AAC; [6]). MS input is phasic at theta rhythm and is on for 125 ms during the retrieval phase.

Recent results have elaborated on the timing dependence of LTP by showing that long-term plasticity depends critically on the millisecond timing of pre- and postsynaptic spikes. Typically, if the presynaptic cell fires an AP a few milliseconds before the postsynaptic cell, LTP is produced, whereas the opposite temporal order results in LTD, a notion called spike timing-dependent plasticity (STDP). Interestingly, the rules of STDP vary widely within brain region, cell, and synapse type.

During storage an STDP learning rule (based on the experimental findings by [17]) was applied at CA3-AMPA synapses on PCs medial SR dendrites, where presynaptic CA3 input spike times were compared with the postsynaptic voltage response to determine an instantaneous change in the peak synaptic conductance.

$$g_{\text{peak}}(t) = g^0_{\text{peak}} + A(t) \tag{4.1}$$

with

$$A(t) = \begin{cases} A(t-1)\left(1 - d\,\frac{e^{(\Delta t - M_d)^2/2V_d^2}}{V_d\sqrt{2\pi}}\right) & \text{if } \Delta t < 0 \\ A(t-1) + \left(g^{\max}_{\text{peak}} - g^0_{\text{peak}} - A(t-1)\right)\, p\, e^{-\Delta t/\tau_p} & \text{if } \Delta t > 0, \end{cases} \tag{4.2}$$

where $\Delta t = t_{\text{post}} - t_{\text{pre}}$. $M_d = -22ms$, $V_d = 5ms$, $\tau_p = 10ms$ are set in order to reproduce the critical time window found by [17], g^0_{peak} is the initial peak conductance, $g^{\max}_{\text{peak}}$ is the maximum value which g can reach. The parameters p and d are chosen in such way that, in the same time of the protocol of [17], i.e. 16 ms, the conductance peak of synapses under plasticity lies in a range near to maximum value.

In addition, during storage the CA3-AMPA synaptic conductance suppression by the putative $GABA_B$ inhibition present during this phase was implemented simply by scaling so that effective conductance g' was:

$$g' = g_s \times g, \tag{4.3}$$

where g_s is the scaling factor (set to 0.4). During recall, g' was simply equal to g.

4.2. Pattern storage and recall

Hasselmo et al. [7, 8] have hypothesized that the hippocampal theta rhythm (4–7 Hz) contributes to memory formation by separating storage and recall into different functional subcycles. Recent experimental evidence has shown that different types of inhibitory interneurons fire at different phases of the theta rhythm [11, 12, 25]. Here, we demonstrate how the recall performance of previously stored patterns is affected by the presence/absence of various types of inhibitory interneurons, which fire at different phases of the simulated theta rhythm.

A set of patterns are stored by generating a weight matrix based on the sequence of the applied STDP rule. The initial weight matrix is chosen in such a way that there are no CA1 spikes in the recall phase if in the storage the STDP was not active (the weights being equal initially to 0.45 nS). To test recall of a previously stored pattern, the associated input pattern is applied as a cue in the form of spiking of active CA3 inputs (those belonging to the pattern) distributed within a gamma frequency time window. The entire cue pattern is repeated at gamma frequency (40 Hz). At the same time, 20 EC inputs also fire randomly distributed within a 25 ms gamma window, but with mean activity preceding the CA3 activity by 9 ms. The CA3 spiking drives the CA1 PCs plus the B, AA and BS interneurons. The EC input also drives the B and AA interneurons.

To test pure recall by the CA3 input cue, the EC input is disconnected from the CA1 PCs and no learning takes place at CA3 synapses on CA1 PCs. The CA3 synapses are suppressed during the "storage" phase of theta. Pattern recall only occurs during the "recall" half-cycle. Typical firing patterns of the different cell types across theta cycles are illustrated in Fig. 5, where the phase relationships between neuron's activity can be easily seen.

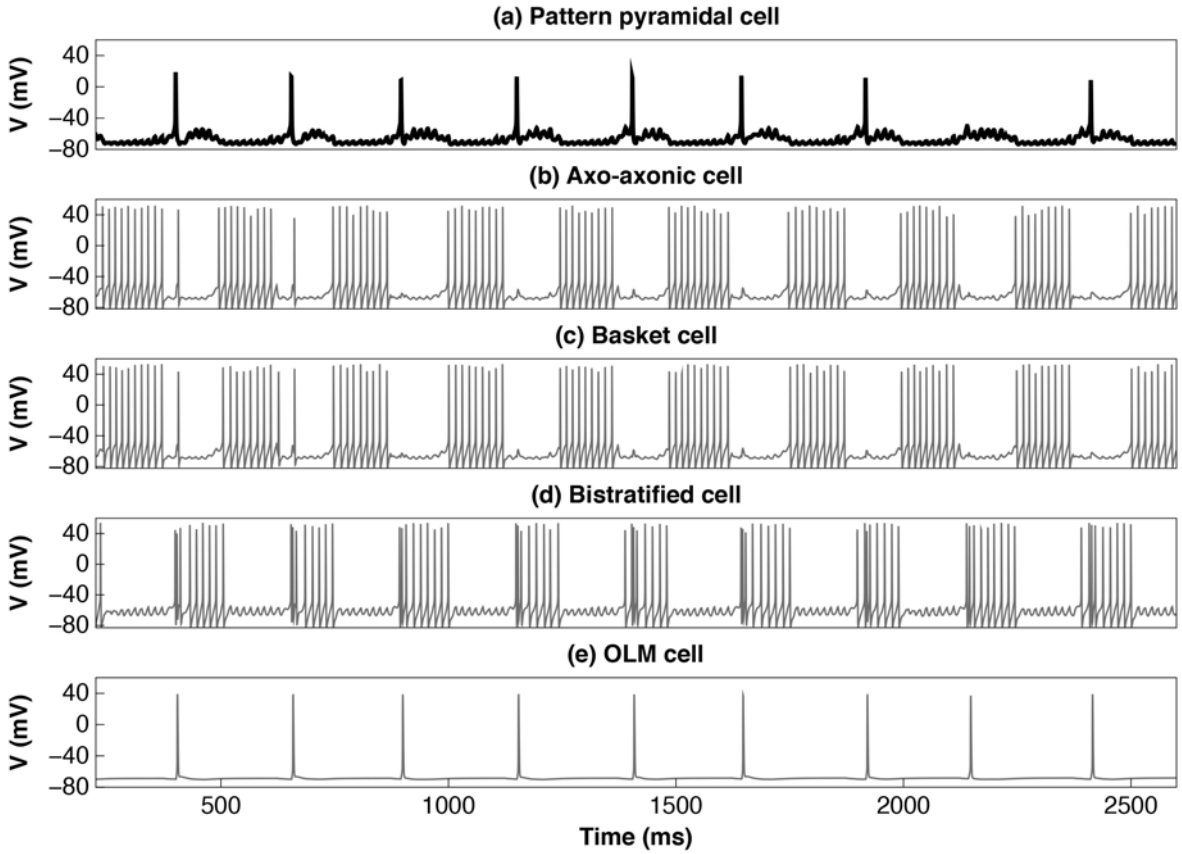

Fig. 5. Voltage response of the different neurons of the network. Example of a PC belonging to the pattern, and each type of inhibitory interneuron, for the recall of one pattern in a set of six.

All simulations were performed using NEURON [9] running on a cluster of 8 nodes with MPI (Message Passing Interface).

4.3. Recall quality

Recall performance is calculated by measuring the CA1 PC spiking activity during a sliding 5 ms time window. For each window a binary vector of length 100 is formed, with entries having a value of 1 if the corresponding PC spikes in the window.

After supplying an input pattern with nP active neurons for storage, the quality of the recall (ranging from 0 to 1) is measured by its correlation with the output pattern, calculated as the normalized dot product:

$$q(P, P') = \frac{\sum_{i=1}^{N} P_i \cdot P'_i}{\sqrt{\sum_{i=1}^{N} \sum_{j=1}^{N} P_i \cdot P'_j}}, \tag{4.4}$$

where P is the input pattern, P' the output pattern and N the total number of CA1 neurons.

In general, a higher quality reflects a better recall. To be more precise, $q = 1$ indicates that the input and output patterns are the same, while $q = 0$ indicates either that the output has no active CA1s in common with the input, or that all cell are quiescent. A pattern was considered correctly recalled if its recall quality q was above a threshold Th. This value corresponds to the quality of the recall of an output pattern in which all neurons are active. For our network ($N = 100$, $nP = 20$), $Th = \frac{20}{\sqrt{20 \times 100}} = 0.4472$.

5. RETRIEVAL OF ULTRAMETRIC PATTERNS IN THE CA1 NETWORK

In order to understand the results of the model of the storage/recall process we have to analyze the meaning of the simulations.

This is because usually when such processes are analyzed it is natural to use the concepts of associative memory that we have described in Section 2. For example, the retrieval is done presenting a certain pattern of activity to the neural system, this pattern coinciding with the bits of some stored pattern with exception of a given percent of the number of total bits, this percentage representing the error. Then the network dynamics transforms this perturbed pattern in the pattern without perturbation, apart for a small percent of bits. This is the standard way of approaching the retrieval in the theory of associative neural networks.

But this approach cannot be applied directly to the case of CA1 neurons. First the storage and retrieval are not separated but are performed sequentially in a series of storage-recall cycles, second we cannot be sure that a certain neuron is active since the initial condition is assigned to that neuron by means of a stochastic input from CA3 and EC neurons, so the neuron is in the required active state only with some probability. The third problem is that the reaction of a neuron to a given input depends mostly on the excitability of such neuron, this is quite different situation from the simple sign dynamics of the Hopfield model.

Cases in which there are no spikes over an entire theta recall half-cycle are termed “silent cycles”. Also, since the storage-retrieval is done on a sequence of a certain number of cycles, it may be that the neuron fires in some cycles and can be silent in other cycles.

Using a sufficiently large statistics it is possible to take into account all these cases. In general our attitude is that if the neuron is silent for all the 9 cycles then we simply consider that the presentation of the pattern to the network has failed. In all the other cases we have to consider the average of the quality over the recall cycles and the form of the histograms of the recall quality. Furthermore we are not studying the convergence of a perturbed pattern to the original one, but simply the stability of the activity pattern under the action of the neural dynamics. We present here the first results of the simulations.

In Fig. 6 we show the recall of one pattern in a set of six ultrametric patterns (in the sense of the hierarchy introduced before) stored by the network. This is the case already described in Section 3, thus the Rammal index of the deviation from ultrametricity is 0.0079. The points represent the spiking neurons. In the upper part of the picture the activity of the input neurons is shown, while in the middle the CA1 neurons spiking is represented. In the lower part the retrieval quality is depicted. The gray highlighted areas are the theta half-cycles in which recall occurs. The red pattern is the input pattern, shown for clarity.

We have then simulated the storage and retrieval of groups of 6 patterns with different ultrametric structures.

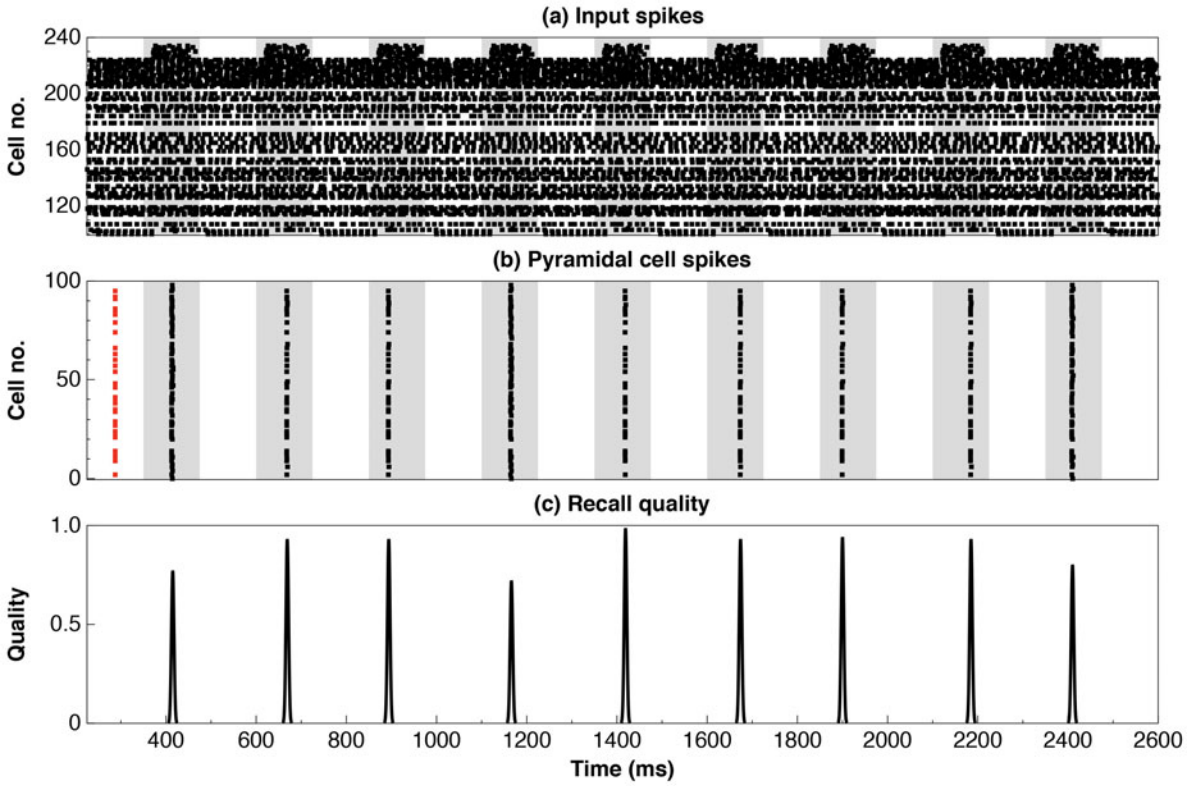

Fig. 6. Raster diagram of the retrieval of a pattern with Rammal index 0.0079. The CA3 input is cueing a pattern (in red) in a stored set of six. EC input is present to drive the inhibitory interneurons, but is disconnected from the CA1 PCs, so that recall is purely due to the CA3 input cue. Nine 125 ms recall half-cycles are shown (the light gray areas). (a) Raster plot showing the septal (*top* 10), EC (*next* 20), CA3 (*next* 100) and interneurons (*bottom* 5) spikes. (b) Raster plot showing CA1 PC activity – virtually the only active cells are those belonging to the stored pattern. (c) Recall quality.

The histograms in Fig. 7 show the quality recall for each pattern belonging to the group with Rammal index 0.064 and Lerman index 0.11, in 9 cycles of storage and recall. All histograms are thus constructed on 9 values of the retrieval quality for each pattern during each of the 9 cycles. So the statistics is partial because we should vary also the inputs from CA3 and EC in order to have the full informations.

The histograms are different for each pattern and this can be explained if one considers that the stochastic input from CA3 and EC neurons have different effects on the different CA1 neurons due to the randomness of the input.

In our model we can also simulate the effect of the degeneration of Alzheimer's disease with the introduction of impaired synapses, in a similar way as we did in the past [3]. In that work we have also introduced the positive influence of the CREB overexpression on the neural excitability. We investigated if the action of CREB can compensate the decrease of the retrieval quality due to the impaired synapses.

In Fig.s 8-9 we show the recall quality for systems of pattern with different degrees of deviation from ultrametricity, the latter being evaluated respectively with the Lerman and the Rammal indices.

We see that the quality oscillates in a small interval when the deviation from ultrametricity increases, both in the Control and Alzheimer cases, i.e. if the number of impaired synapses increases. Of course in the Alzheimer case the quality of the recall is worse than in the Control case. But if we introduce CREB, the retrieval quality for the Alzheimer case is better than in the Control case. This holds for both indices of deviation from ultrametricity. We have also seen, as expected, that under the CREB action there are no silent states, which simplifies the statistics.

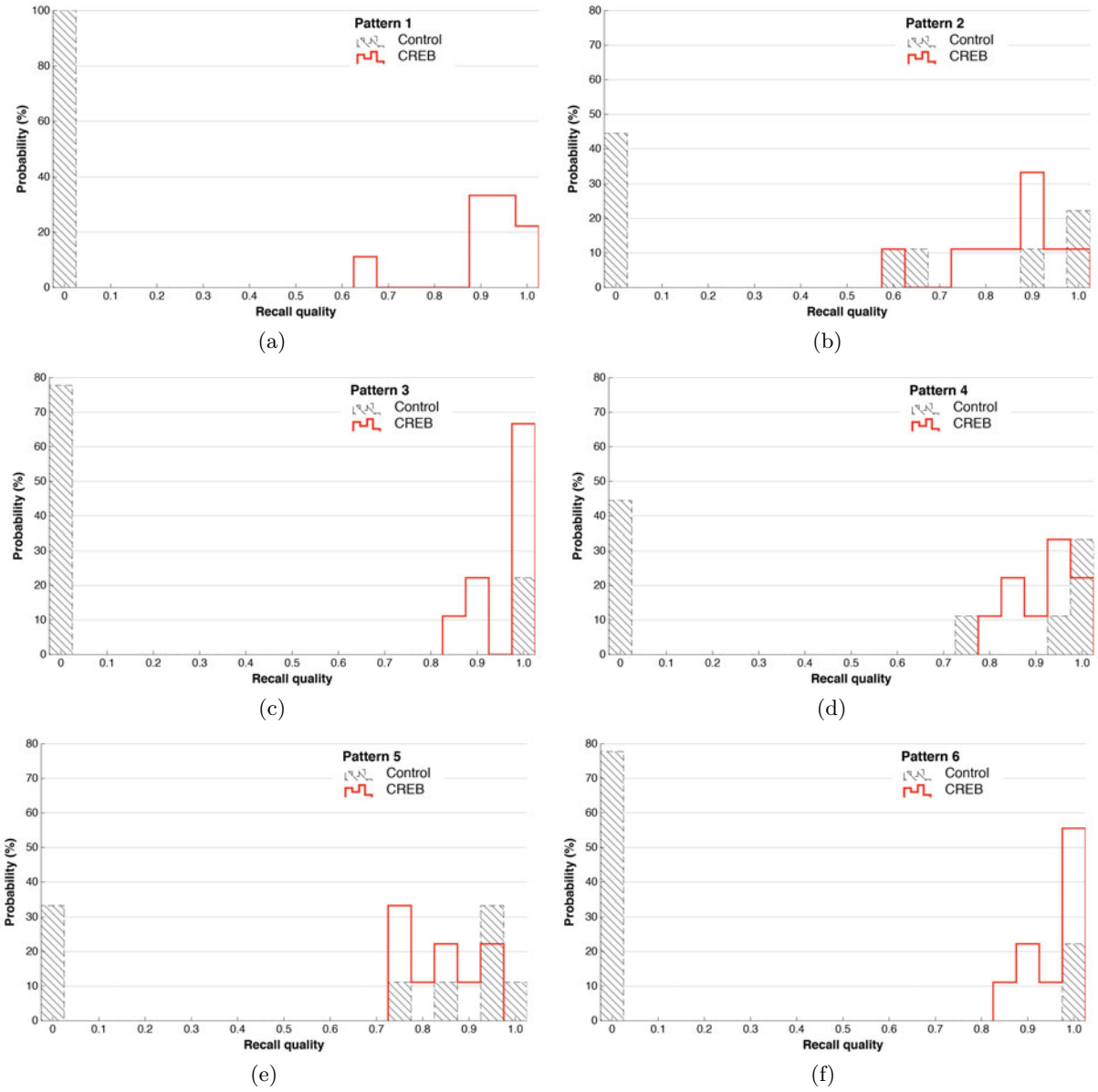

Fig. 7. Histograms of the recall quality of the patterns belonging to a group of 6, with Rammal index 0.064 and Lerman index 0.11.

5.1. Conclusions

In conclusion, this first set of simulations gives interesting results, that have to be confirmed with a larger set of data and statistics. An unsolved question remains the presence of silent states during the recall cycles.

Following the ideas of [3] we have to choose between two different ways to measure the recall quality, excluding (Q1) or including (Q2) silent cycles. Q1 is defined as the average of the quality values obtained from all time windows with at least 1 spike, i.e. silent theta recall hemicycles were not considered (as in [5]). Q2 includes silent cycles, which contribute to the average quality with a zero value. Note that these two measures highlight different aspects of the output, Q1 focusing more on the quality of the output patterns, whereas Q2 is more sensitive to their quantity.

Bianchi et al. [3] have found that Q1 is more consistent with experimental findings on the activity of CA1 neurons, although this has not been investigated yet in the case of ultrametric patterns. This problem will arise only in the Control case since, as we have already observed, CREB increases neuron's excitability and there are no silent states in this case. With an extended statistics it is also

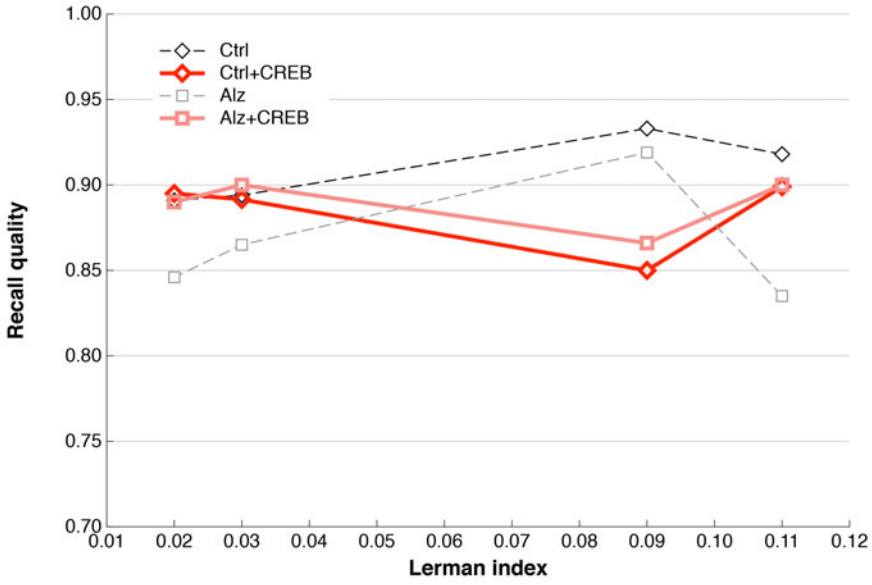

Fig. 8. Behavior of the average recall quality both in the Control case and with impaired synapses (Alz) as a function of the Lerman index, with and without CREB. The recall quality oscillates in a small interval with the increase of the deviation from ultrametricity.

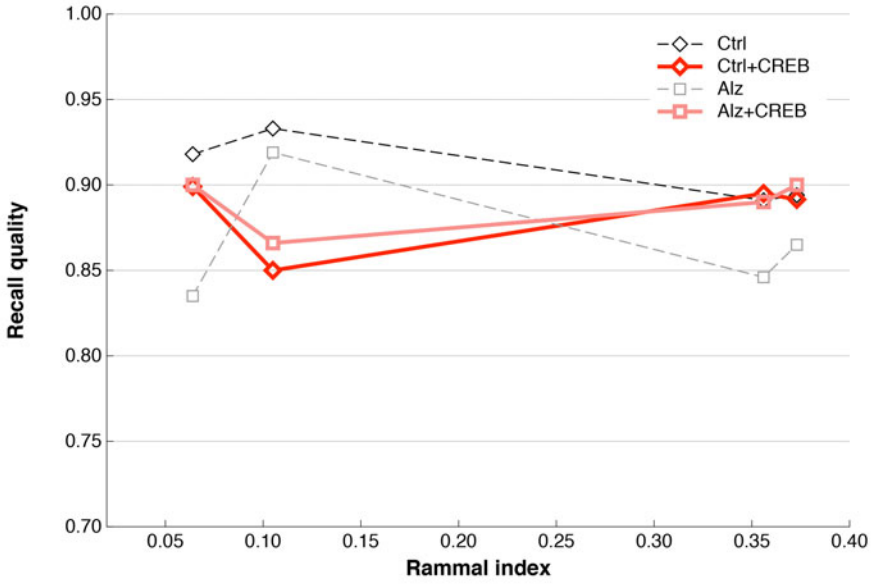

Fig. 9. Behavior of the average recall quality both in the Control case and with impaired synapses (Alz) as a function of the Rammal index, with and without CREB. The recall quality oscillates in a small interval with the increase of the deviation from ultrametricity.

possible to study the histogram of the recall quality for each pattern and we will check the degree of randomness of the silent states. If the variance is large we could infer that the silent states have a random nature connected probably with the way we force the neuron to be in the required initial state.

The other steps will be to extend this analysis to the study of critical capacity. This implies the study of the quality of recall for networks with increasing number of patterns and neurons. The dependence of the critical capacity on CREB will give a possibility to give the meaning of

associative memory to the memory function of the hippocampus and this can create an alternative way to consider also the diseases of the memory.

So this study gives preliminary answers to the question of the sensitivity of the recall quality to the degree of ultrametricity of the group of stored patterns. If the number of patterns is small there are no big problems to construct a group with a given degree of ultrametricity, but when the number is large this task is not trivial.

The question about ultrametricity is important because it is connected with the existence of categories in the information stored in memory. The construction introduced in [1] (and described in Section 2) is somehow limited by the assumption of independence of the bits of the pattern, while the preorder measured by the Rammal and Lerman indices is more general and more similar to the information processed by the brain.

Finally the analysis of the memory of a realistic set of patterns gives more interest in the simulation of the Alzheimer's disease.

REFERENCES

1. D. Amit, *Modeling Brain Function: The World of Attractor Neural Networks* (Cambridge Univ. Press, Cambridge, 1989).
2. D. Amit, H. Gutfreund and H. Sompolinsky, "Storing infinite numbers of patterns in a spin-glass model of neural networks," Phys. Rev. Lett. **55**, 1530–1533 (1985).
3. D. Bianchi, P. De Michele, C. Marchetti, B. Tirozzi, S. Cuomo, H. Marie, and M. Migliore, "Effects of increasing CREB-dependent transcription on the storage and recall processes in a hippocampal CA1 microcircuit," Hippocampus (2013).
4. D. Bianchi, A. Marasco, A. Limongiello, C. Marchetti, H. Marie, B. Tirozzi and M. Migliore, "On the mechanisms underlying the depolarization block in the spiking dynamics of CA1 pyramidal neurons," J. Comput. Neuroscience **33** (2), 207–225 (2012).
5. V. Cutsuridis, S. Cobb and B. P. Graham, "Encoding and retrieval in a model of the hippocampal CA1 microcircuit," Hippocampus **20** (3), 423–446 (2010).
6. T. Freund and M. Antal, "Gaba-containing neurons in the septum control inhibitory interneurons in the hippocampus," Nature **336** (6195), 170–173 (1988).
7. M. Hasselmo, C. Bodelón and B. Wyble, "A proposed function for hippocampal theta rhythm: separate phases of encoding and retrieval enhance reversal of prior learning," Neural Comput. **14** (4), 793–817 (2002).
8. M. Hasselmo, J. Hay, M. Ilyn and A. Gorchetchnikov, "Neuromodulation, theta rhythm and rat spatial navigation," Neural Netw. **15** (4), 689–707 (2002).
9. M. Hines and N. Carnevale, "The neuron simulation environment," Neural Comput. **9** (6), 1179–1209 (1997).
10. J. Hopfield, "Neural networks and physical systems with emergent collective computational abilities," Proc. Nat. Acad. Sci. **79** (8), 2554–2558 (1982).
11. T. Klausberger, L. Márton, A. Baude, J. Roberts, P. Magill and P. Somogyi, "Spike timing of dendrite-targeting bistratified cells during hippocampal network oscillations in vivo," Nature Neurosci. **7** (1), 41–47 (2004).
12. T. Klausberger and P. Somogyi, "Neuronal diversity and temporal dynamics: the unity of hippocampal circuit operations," Science **321** (5885), 53–57 (2008).
13. H. Marie, W. Yu. X. Morishita, N. Calakos and R. C. Malenka, "Generation of silent synapses by acute in vivo expression of CaMKIV and CREB," Neuron **45** (5), 741–752 (2005).
14. W, McCulloch and W, Pitts, "A logical calculus of the ideas immanent in nervous activity," Bull. Math. Biol. **5** (4), 115–133 (1943).
15. M. Mézard, G. Parisi and M. Virasoro, *Spin Glass Theory and Beyond* (World Scientific, Singapore, 1987).
16. F. Murtagh, "A survey of recent advances in hierarchical clustering algorithms," Comput. J. **26** (4), 354–359 (1983).
17. M. Nishiyama, K. Hong, K. Mikoshiba, M. Poo and K. Kato, "Calcium stores regulate the polarity and input specificity of synaptic modification," Nature **408** (6812), 584–588 (2000).
18. L. Pastur, M. Shcherbina and B. Tirozzi, "The replica symmetric solution of the Hopfield model without replica trick," J. Stat. Phys. **74** (5/6), 1161–1183 (1994).
19. P. Poirazi, T. Brannon and B. Mel, "Arithmetic of subthreshold synaptic summation in a model CA1 pyramidal cell," Neuron **37** (6), 977–987 (2003).

20. P. Poirazi, T. Brannon and B. Mel, "Pyramidal neuron as two-layer neural network," Neuron **37** (6), 989–999 (2003).
21. R. C. Prim, "Shortest connection networks and some generalizations," Bell System Tech. J. **36** (6), 1389–1401 (1957).
22. V. Santhakumar, I. Aradi and I. Soltesz, "Role of mossy fiber sprouting and mossy cell loss in hyperexcitability: a network model of the dentate gyrus incorporating cell types and axonal topography," J. Neurophysiol. **93** (1), 437–453 (2005).
23. F. Saraga, C. Wu, L. Zhang and F. Skinner, "Active dendrites and spike propagation in multi-compartment models of oriens-lacunosum/moleculare hippocampal interneurons," J. Physiol. **552** (3), 673–689 (2003).
24. A. Soleng, M. Raastad and P. Andersen, "Conduction latency along CA3 hippocampal axons from rat," Hippocampus **13** (8), 953–961 (2003).
25. P. Somogyi and T. Klausberger, "Defined types of cortical interneurone structure space and spike timing in the hippocampus," J. Physiol. **562**, 9–26 (2005).